Ku-BAND RECEIVER FRONT-END USING MIC TECHNOLOGY

C. M. Krowne, F. A. Marki, E. J. Crescenzi, Jr.
Watkins-Johnson Company
3333 Hillview Avenue, Stanford Industrial Park
Palo Alto, California 94304

Abstract

The development of a Ku-band receiver front-end using microwave integrated circuit technology is described. The front end elements, including a GaAs FET RF balanced amplifier stage, an image reject mixer, and a varactor controlled GaAs FET oscillator are integrated in a very small simple hermetic package. Electrical design details are presented for the varactor controlled FET oscillator development.

Introduction

Small remotely piloted vehicles (RPV's) require ultra-miniature and highly efficient electronic components because of stringent limitations on payload size. This requirement emphasizes the urgent need for a fresh and novel approach to microwave receivers utilizing innovative philosophy and new components. This paper addresses this problem.

Here we discuss an effort to produce a fully integrated receiver front-end using microstrip integrated circuit technology. The receiver operates at 15 GHz with a bandpass of 1 GHz.

The elements which are integrated include a preselector filter, a balanced single stage GaAs FET amplifier, a Schottky diode image reject mixer, and a varactor tuned GaAs FET oscillator. These components are integrated and enclosed in a very small (0.65 by 0.25 by 1.7 inches) hermetically sealed module (Figure 1).

Receiver Front End Design

This receiver module design is the result of general requirements to achieve RF performance goals with minimum size and complexity. The balanced FET input amplifier[1,2] serves three functions: 1) reduction of overall noise figure by preamplification (typically 5.0 dB gain and 5.0 dB noise figure), 2) establishment of terminal VSWR of about 1.5:1 for interface with both the filter and mixer, and 3) achievement of a reverse isolation of typically 20 dB so that local oscillator (L.O.) reradiation is reduced. Choice of the number of stages of RF amplification is a tradeoff between noise figure and cost. The balanced silicon Schottky diode image reject mixer[3] converts the RF input signal to an IF of 300 MHz, while rejecting image signals and amplifier output image noise by about 25 dB. The balanced nature of the mixer also provides rejection of the $2f_L - 2f_R$ spurious product and rejection of the L.O. signal at the mixer RF input port by about 25 to 30 dB. The mixer design chosen is driven on the L.O. port via an interdigitated quadrature hybrid[4] which maintains a moderately low (1.5:1) VSWR (to first order independent of L.O. power) at the L.O. input port, which allows direct interface of the oscillator with the mixer.

The oscillator is required to deliver about +5 dBm minimum of power to the mixer, and to be electronically tunable over a 1 GHz bandwidth. The design presented here involves a new circuit topology with transmission line feedback for optimization of the characteristics of a low cost GaAs FET at 15 GHz.

Oscillator Design

The design of the 15 GHz FET oscillator has involved evaluation of several circuit topologies with regard to achieving the necessary conditions for oscillation over the desired 1 GHz frequency range. Circuit topologies were restricted to those amenable to microstrip realization. Below we first outline a fixed tuned oscillator design approach which is then extended to include tuned oscillator design.

In terms of reflection coefficients, the basic conditions of oscillation are[5]

$$|\Gamma_a| > \frac{1}{|\Gamma_r|} \quad , \tag{1}$$

and

$$\angle\Gamma_a + \angle\Gamma_r = 0 \quad . \tag{2}$$

Figure 2 shows an oscillator in block diagram form. It contains a resonator microstrip element, an active network which uses a FET, an output matching network, and the load. The load here, of course, is a mixer with $\Gamma_L \approx 0$ (50 Ω system). In our illustration here of the oscillator design approach we make three simplifying assumptions which do not limit the generality of the conclusions to follow: 1) the resonator reflection coefficient is taken $|\Gamma_r| = 1$; 2) small signal s-parameters are utilized to characterize the GaAs FET's used in the active network $(\Gamma_a = s_{11}')$; and 3) $\Gamma_m = 0$. The focus is on the active network. The circuit topology of the active network is made to maximize $|\Gamma_a|$ which is taken as a figure of merit for oscillation stability. Condition (2) is met by adjusting the length of a short circuited shunt stub (SCSS) transmission line length ℓ to ground once $\angle s_{11}'$ is known. For a FET (such as an NEC 244 or a DXL 502) in common source configuration, $|\Gamma_a| = |s_{11}| < 1$. Figure 3 shows the active circuit topology and the Smith Chart plotting s_{11}' (mapped from s_{11} using computer aided design methods) under varying SCSS lengths ℓ off the source of the FET. Here we have taken $s_{11} = 0.53 \angle -179^\circ$ from an actual case. Notice that for capacitive source-to-ground feedback ($\ell = 0.25$ inch in

air), $|\Gamma_a| = |s_{11}| > 1$. Since $|s_{11}| = 1.07$ at this point, only marginal oscillatory operation is expected. In order to increase $|\Gamma_a|$, a transmission line drain-to-gate feedback element has been added as seen in Figures 4(a) and 4(b) which respectively show the circuit topology and the Smith Chart for varying feedback lengths ℓ. For $0.065 \lesssim \ell \lesssim 0.37$ in., $|s_{11}| > 1$. At $\ell = 0.1$ in. (a point close to the maxima), $|s_{11}| \approx 1.79$. Figure 4(b) also demonstrates that there are three arc regions, (0.35, 0.5 in.), (0.7, 0.07 in.), and (0.08, 0.25 in.), where approximately simple mappings into arcs of circles occur due to the bilinearity property. This behavior implies that for these arcs we are mapping circles of constant resistance and varying reactance or circles of varying resistance and constant reactance.

Figure 5 shows the experimental results for P_{osc} dependence on the Drain-to-Source DC bias V_{DS} under two bias current I_{DS} conditions; $I_{DS} = 15$ mA and 20 mA. Turn-on indicates the bias at which oscillatory behavior commences. Figure 5 indicates that for $V_{DS} \gtrsim 2.7$ V, $P_{osc} \gtrsim 7$ dBm which is sufficient to drive the mixer.

Varactor Oscillator

It is only a short step from the fixed tuned oscillator outlined above to a varactor controlled oscillator. Here, however, one needs to solve Eqs. (1) and (2) in the frequency domain to obtain the bandwidth Δf_o over which the center frequency f_o varies for varactor bias control:

$$|\Gamma_a(f)|\,|\Gamma_r(f)| > 1 \quad , \tag{3}$$

and

$$\angle\Gamma_a(f) + \angle\Gamma_r(f) = 0 \quad . \tag{4}$$

For a particular varactor voltage V_v [or the varactor capacitance $C_v(V_v)$], there is a solution to Eqs. (3) and (4): $f_o = f_o(C_v)$. It has been found by CAD techniques that if the varactor is placed in series with the gate SCSS, Δf_o's in excess of 1 GHz result. The final varactor tuned oscillator circuit topology is shown in Figure 6a, and the actual circuit is shown in Figure 6b. Frequency as a function of varactor bias is given in Figure 7 for a DC drain supply bias setting $V_s = 8$V. The final circuit (Figure 6b) is readily realized with thin film microstrip techniques. The circuit construction is substantially simpler than that of the amplifier since the source is grounded through a resonator element and close proximity of the ground plane to the FET device is not necessary.

Receiver Front-End Module

The assembled receiver front-end module is shown in Figure 8. It includes an input RF filter, balanced GaAs FET amplifier, image reject mixer, and GaAs FET varactor tuned oscillator. All substrates are brazed to a Kovar carrier using Au-Sn eutectic braze. The filter, amplifier, and mixer are realized on fused silica substrate, whereas the oscillator employs alumina (due to superior thermal conductivity). The circuit frame is gold plated Kovar with fused glass hermetic RF feedthru's, and a top cover is parallel seam welded to the frame to achieve total package hermeticity. Semiconductor devices employed include: 1) NEC 388 GaAs FET's for the RF amplifier; 2) Dexcel 502 GaAs FET and Alpha Industries type CVH-2030 abrupt-junction silicon tuning diode for the oscillator; and 3) Alpha Industries D5600A Schottky beam lead diodes in the mixer.

The RF front-end module electrical results are given in Figure 9. Performance varies depending on particular input filter characteristics, so the electrical parameters of Figure 9 are for the input filter replaced by a straight through (input to amplifier) 50 ohm microstrip line. Noise figure (single side band) is approximately 7.5 dB overall, and a net module loss of about 1.5 dB is incurred because the mixer loss exceeds amplifier gain by that amount. In a typical application, the necessary total gain is achieved by use of a high gain IF (300 MHz) amplifier. The RF frequency is 300 MHz below that shown in Figure 7. Although oscillator power into the mixer cannot be directly measured for the completed module, mixer performance allows inference of about +5 dBm to +10 dBm. The module input VSWR and oscillator leakage level out of the input port are also given in Figure 9.

Conclusions

A 15 GHz receiver front-end module has been designed and constructed exclusively utilizing thin film microstrip technology. The complete circuit is contained in a simple 5 cm^3 hermetic module. The design of a key circuit element, the GaAs FET 15 GHz oscillator with varactor tuning over a 1 GHz bandwidth, has been presented. Essential to the oscillator realization is the incorporation of transmission line feedback from drain-to-gate, with the gate resonator including a series connected varactor. The front-end module performance is considered to demonstrate the feasibility of direct microstrip interface of these circuit elements in a novel low cost hermetic package.

Acknowledgements

The authors would like to thank Mr. Richard W. Oglesbee of Watkins-Johnson Company for his valuable contribution in circuit fabrication and microwave measurements.

References

1. M. G. Walker and E. J. Crescenzi, Jr., "A 12-15 GHz High Gain Amplifier Design Using Submicron Gate GaAs Field Effect Transistors," IEEE MTT-5 Intern. Micro. Symp. Dig., p. 107, June 1976.

2. M. G. Walker, F. A. Marki, and H. M. Abramowitz, "MESFET Amplifiers Go To 18 GHz," Micro. Sys. News, April/May 1976.

3. James B. Cochrane and Ferenc A. Marki, "Thin Film Mixers," Microwaves, pp. 34-40, March 1977.

4. J. Lange, "Interdigitated Stripline Quadrature Hybrid," IEEE Trans. Microwave Theory Tech. (Corresp.), Vol. MTT-17, pp. 1150-1151, December 1969.

5. C. M. Krowne, "Network Analysis of Microwave Oscillators Using Microstrip Transmission Lines," Electr. Letts., Vol. 13, No. 4, pp. 115-117, 17th February 1977.

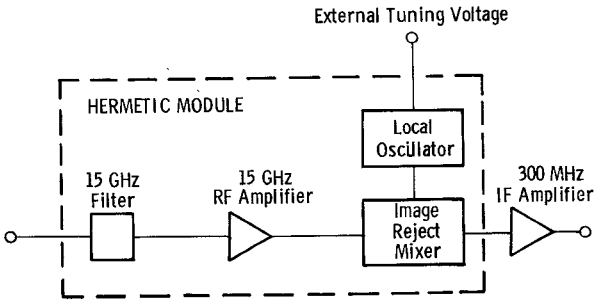

Fig. 1 Ku-band receiver front-end module block diagram.

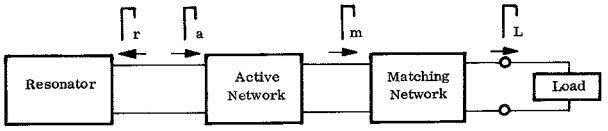

Fig. 2 Oscillator block diagram.

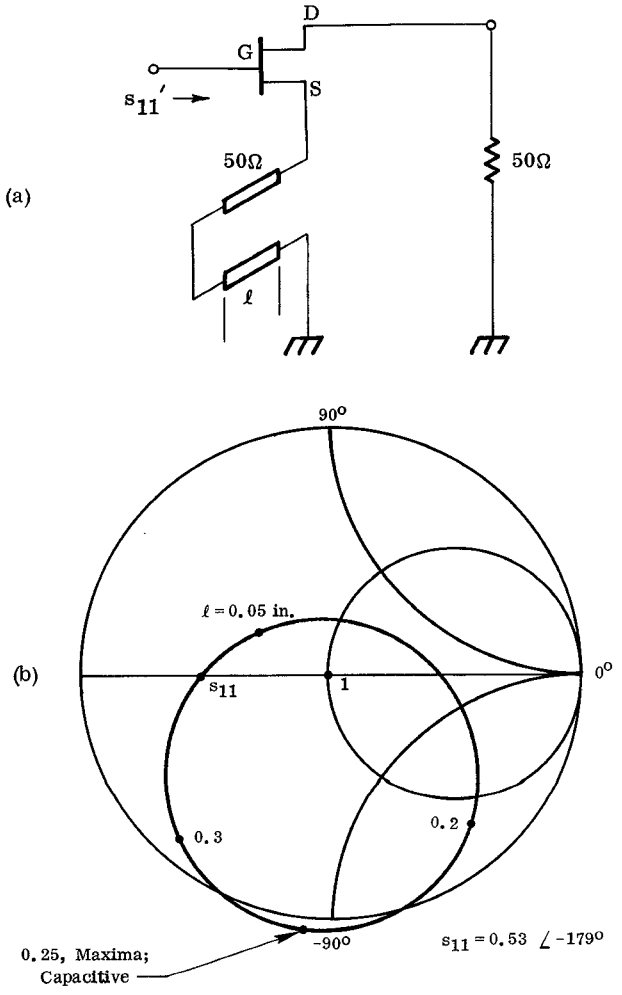

Fig. 3 Common source configuration with source-to-ground feedback and resultant reflection coefficient: (a) RF circuit topology; (b) s_{11}'.

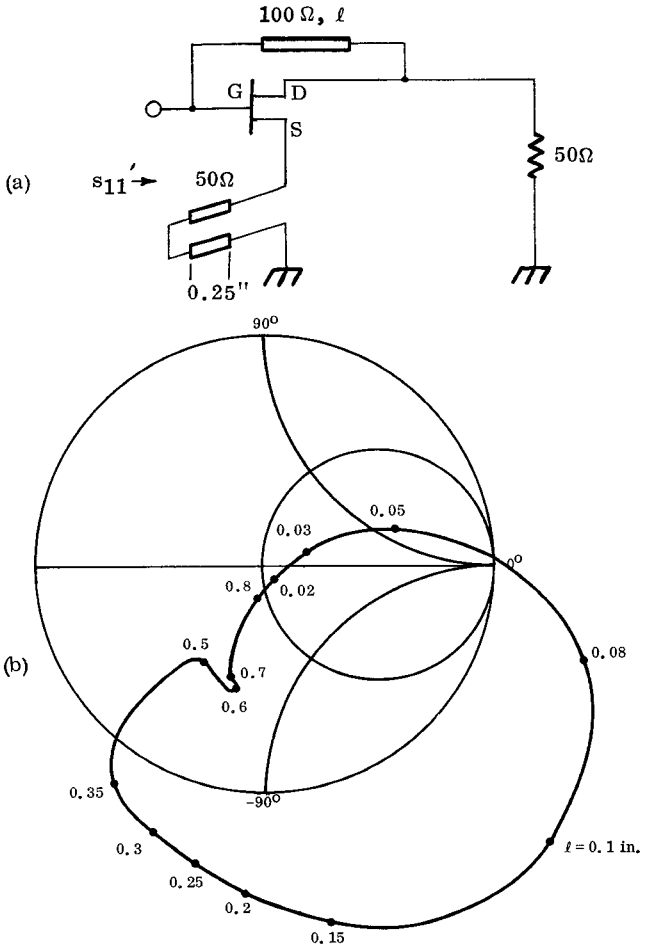

Fig. 4 Common source configuration with source-to-ground and drain-to-gate feedback and resultant reflection coefficient: (a) RF circuit topology; (b) s_{11}'.

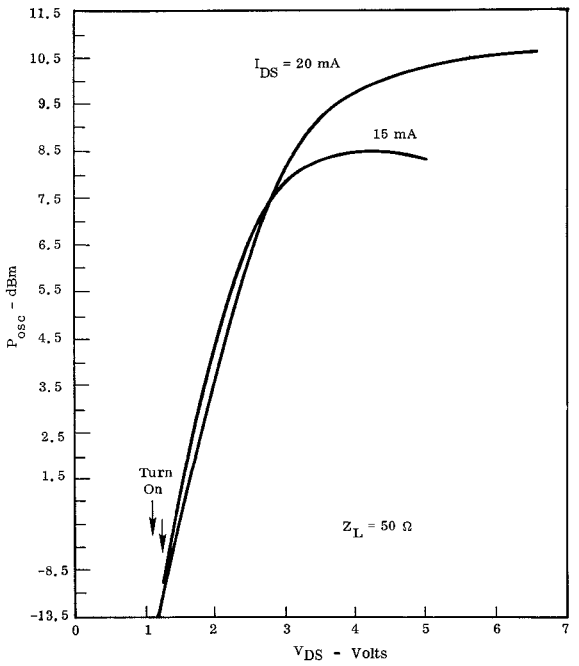

Fig. 5 Fixed tuned oscillator output power P_{osc} as a function of the drain-to-source voltage V_{DS} (oscillator frequency is nominally 15 GHz).

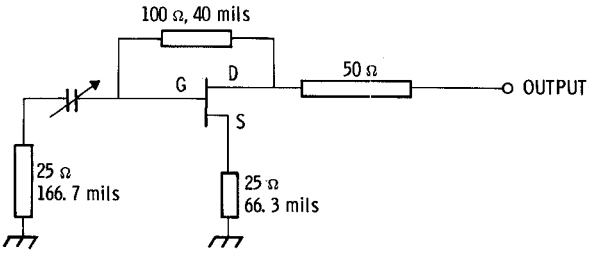

Fig. 6a RF varactor tuned oscillator circuit topology. Transmission line lengths are given for 15 mil thick alumina substrate.

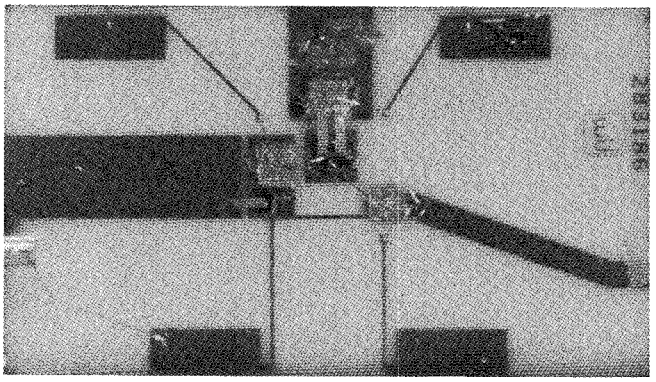

Fig. 6b Varactor oscillator thin film circuit.

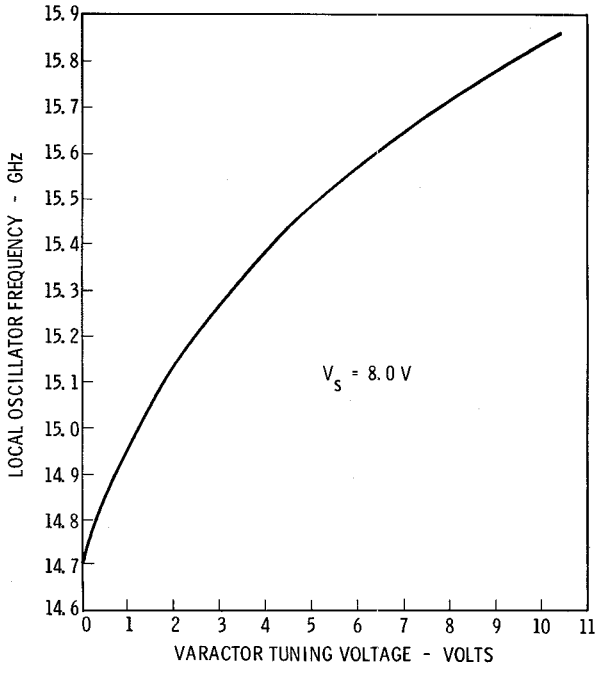

Fig. 7 Local oscillator frequency f_o versus varactor voltage (note: f_o measured with oscillator directly interfaced with the thin film mixer of Fig. 8).

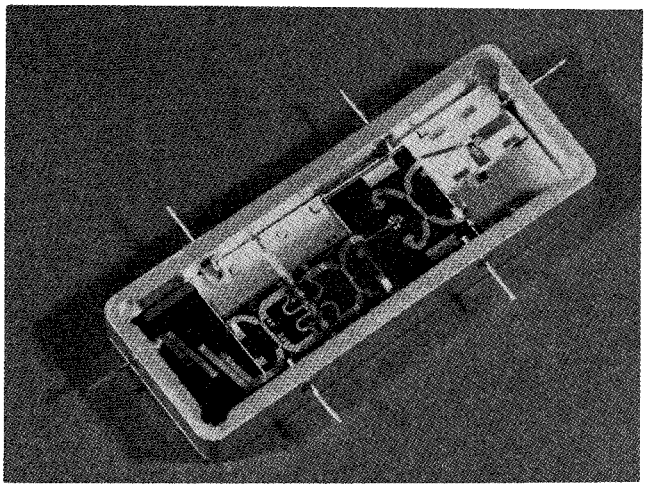

Fig. 8 15 GHz receiver front-end hermetic module (0.65 by 0.25 by 1.70 inches).

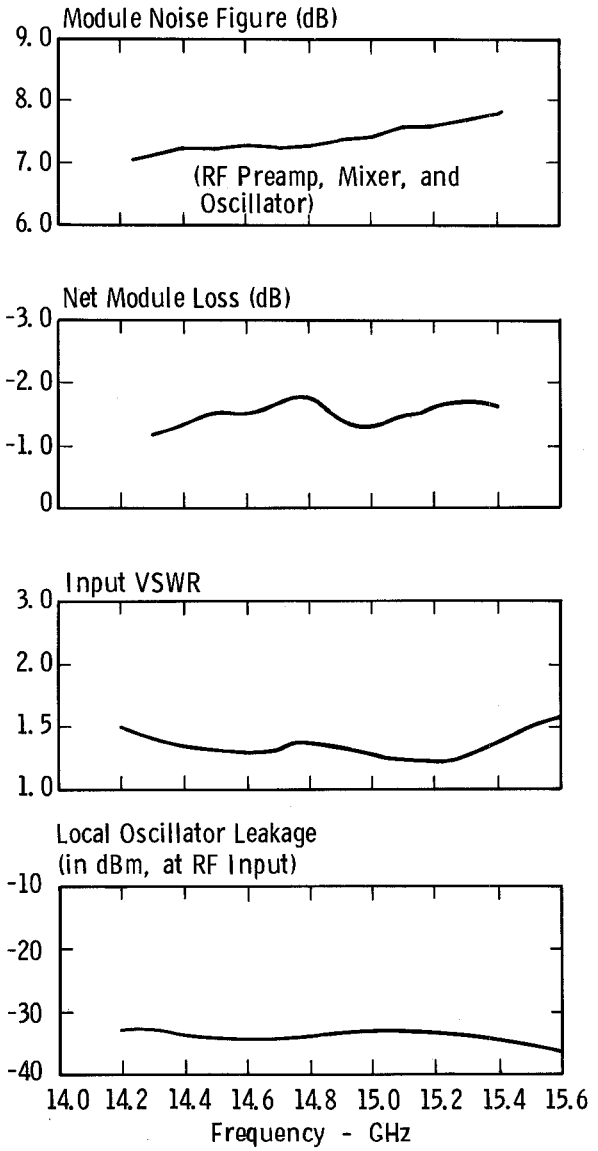

Fig. 9 Ku-band receiver module noise figure, loss, input VSWR, and local oscillator RF input leakage versus RF frequency.